Colloid Polym Sci 274:350–355 (1996)

ORIGINAL CONTRIBUTION

Th. Hack
V. Abetz
M. Stamm
D.W. Schubert
K. Mortensen
W. Siol

Spinodal decomposition of a polystyrene/poly(cyclohexyl acrylate-stat-butyl methacrylate) blend

Received: 11 October 1995
Accepted: 17 November 1995

Th. Hack · M. Stamm · D.W. Schubert
Max-Planck-Institut für Polymerforschung
Postfach 31 48
55021 Mainz, FRG

Dr. V. Abetz (✉)
Institut für Organische Chemie
Johannes-Gutenberg-Universität Mainz
Postfach 39 80
55099 Mainz, FRG

K. Mortensen
Department of Solid State Physics
Post Office Box 49
Riso National Laboratory
Post Office Box 49
4000 Roskilde, Denmark

W. Siol
Firma Röhm GmbH
Postfach 4242
64201 Darmstadt, FRG

Summary The dynamics of spinodal decomposition (SD) after a temperature jump from a kinetically formed single phase state into the unstable part of the two-phase region has been studied with a blend of polystyrene and poly(cyclohexyl acrylate-stat-butyl methacrylate). The time evolution of the structure factor has been examined by small-angle neutron and light-scattering techniques. The combination of the different techniques gave access to a wide wave vector and time range covering a large range of length scales. The activation energy of the diffusion process during spinodal decomposition was determined by a scaling analysis of the later stages of SD, because early stages of SD could not be resolved.

Key words Polymer blends – spinodal decomposition – activation energy – scaling analysis – small-angle neutron scattering – double crystal diffractometry – light scattering

Introduction

Most of the technologically important polymer blends are multiphase systems and their properties depend very much on the morphology. Since the morphology is controlled by the way of preparation, it is essential to know the influence of all parameters in the process leading to the phase separated product. While many blends are heterogeneous all over the composition and temperature range, some blends show phase transitions upon changing the temperature. Temperature jumps are convenient and therefore probably the most important way to induce phase transitions which change the morphology of a polymeric multi component system. Two different mechanisms of phase separation are known [1, 2]. Between the coexistence curve and the spinodal curve mixtures are metastable and phase separation starts after a certain amplitude of concentration fluctuation is reached necessary to form a nucleus of the second phase which grows afterwards. This nucleation and growth mechanism leads to irregular shaped morphologies. The other kind of phase separation is observed inside the spinodal curve (i.e., the unstable region) and is called spinodal decomposition (SD). Here no activation energy barrier has to be overcome by the system to initialize the formation of a second phase and phase separation proceeds in a way such that concentration fluctuations increase mainly on a specific length scale (wavelength). This length scale determines the properties of the system and increases with time. Much

work has been done on SD of polymer blends after temperature jumps from the one- into the two-phase region [1–6]. However, if the process of phase separation is not stopped at some time, both kinds of phase separation yield finally the same macroscopically decomposed sample. Stabilisation of the morphology may be achieved for example by vitrification due to an increasing glass transition temperature T_g of one of the phases or by crosslinking, a concept used also in the field of interpenetrating polymer networks [7].

In a previous study we have reported on the phase behaviour of blends of deuterated polystyrene (PS) and poly(cyclohexyl acrylate-stat-butyl methacrylate)s (P(CHA-stat-BMA)) already in detail [8]. These systems show, depending on the composition of the copolymer, a lower critical solution temperature (LCST) or an upper critical solution temperature (UCST). In this study we investigate the kinetics of spinodal decomposition of an incompatible blend (LCST $< T_g$) of PS and P(CHA-stat-BMA), whereby the incompatible blend could be prepared as an initially homogeneous sample below its glass transition temperature (kinetically formed single phase).

In this contribution it will be shown that, although the early stages of SD could not be resolved by experiment for this system, the activation energy of the diffusion process during SD can be obtained from an analysis of the scaling behaviour of the dominating fluctuation wavelength with time during the later stages of SD [9]. Usually the activation energy is obtained from an analysis of the early stages of SD.

Experimental section

Sample preparation

Deuterated polystyrene was obtained by living anionic polymerization (MPI Polymerforschung). The statistical copolymer was obtained by free radical copolymerization (Röhm GmbH). The polymers used in this study are compiled in Table 1. A blend with 50 wt% PS (which does not correspond to the critical composition) is considered in this study and phase separates immediately, when annealed above its glass transition temperature ($T_g = 55\,°C$). The components were dissolved in THF (5% wt) and the solution cast into a Petri dish. The Petri dish was put into a dessicator containing silica-gel and kept at $-30\,°C$ for 10 days. Under these conditions transparent samples were obtained (films with a thickness of around 10 μm for light scattering, and 100 μm for neutron scattering), which were further carefully dried at 60 °C at atmospheric pressure for 24 h and afterwards annealed at the same temperature under vacuum for the same time. For the neutron scattering experiments thicker samples were necessary, so thin films were stapled to give the right thickness of around 1 mm. The single phase behaviour of the thus prepared blend was checked by DSC as will be discussed later.

Differential scanning calorimetry (DSC)

DSC experiments were performed on a Mettler TA4000, using a heating rate of 10 K/min.

Small-angle neutron scattering measurements (SANS)

Measurements were performed with a wavelength of the neutrons of $\lambda = 0.95$ nm at the SANS-instrument of Risø National Laboratory, Denmark (scattering vector range of 0.05–0.3 nm^{-1}). The samples were investigated under atmospheric pressure. Data were corrected for electronic background, container scattering, transmission, sample volume and for the incoherent scattering by subtraction of the scattering profiles of the pure components by standard procedures. Calibration of the scattering profiles was done with the well known differential scattering cross-section of a water sample of 1 mm thickness.

Double crystal diffractometry (DCD)

DCD measurements were performed at GKSS-Laboratory in Geesthacht, Germany. The wavelength of the

Table 1 Characteristic data of the polymers

Polymer	M_W [$\frac{kg}{mol}$]	M_N [$\frac{kg}{mol}$]	$\frac{M_W}{M_N}$	T_g[K]	N^e
PS-d8	99[d]	92[d]	1.07[d]	375	885
$P(CHA_{0.19}$-stat-$BMA_{0.81})$	463[a]	263[b]	1.79[c]	294	4310

[a] light scattering (THF).
[b] membrance osmometry (toluene).
[c] gel permeation chromatography (THF, PMMA-standard).
[d] gel permeation chromatography (THF, PS-standard).
[e] weight average degrees of polymerisation based on monomer volume of styrene.

neutrons was $\lambda = 0.443$ nm and the scattering vector obtained by variation of two perfect silicon single crystals was in the range of 0.001–0.03 nm^{-1}. The sample geometry was similar to the SANS experiments, but due to the long measurement times the thermal treatment of the samples was done outside the DCD instrument, i.e., the samples were annealed for different times at the decomposition temperature and then quenched to the glassy state (room temperature) to freeze the morphology.

Small-angle light scattering (SALS)

SALS measurements were performed with a homemade apparatus where the sample was placed in a microscope hotstage (Lincam). The sample was irradiated from the bottom by a He–Ne-Laser ($\lambda = 632.8$ nm). The scattering pattern of the sample was monitored by a so-called volume scattering screen from Spindler & Hoyer and then registered by a video camera to give a digitized picture. These pictures were radially averaged and corrected for geometric effects, transmission and background according to standard procedures on a computer. Due to the smearing properties of the scattering screen, only the maximum position of the scattered intensity was obtained from the scattering curves and details of the shape of the SALS traces were not discussed [10].

Theoretical background

Since a detailed description of the theory of spinodal decomposition can be found in many publications [1–3], here only those equations are mentioned, which are essential for the analysis of the data. Spinodal decomposition can be divided into different stages. The early stage can be described by the Cahn–Hillard–Cook theory [1–3, 11, 12]. While the amplitude of the concentration fluctuation increases exponentially with time, the wavelength of concentration fluctuation, $2\pi/q_m(0)$, remains constant if thermal fluctuations are negligible:

$$q_m(0) = \sqrt{\frac{D_{app}}{4M\kappa}} = \sqrt{-\frac{1}{4\kappa}\frac{\partial^2 f_m}{\partial \phi_1^2}} \tag{1}$$

M: mobility
D_{app}: apparent interdiffusion coefficient
f_m: mean field free energy of mixing
ϕ_i: volume fraction of component i
κ: gradient energy coefficient (interfacial free energy density) $\kappa = \frac{\sigma^2}{36\phi_1\phi_2}$
σ: average statistical segment length
q: scattering vector $q = (4\pi/\lambda)\sin(\theta/2)$
λ: wavelength of the radiation in the sample
θ: scattering angle.

The mean field free energy is given by the Flory–Huggins–Staverman theory [13–15] and its second derivative is related to the inverse structure factor at $q = 0$:

$$\frac{\partial^2 f_m}{\partial \phi_1^2} = \frac{1}{N_1\phi_1} + \frac{1}{N_2\phi_2} + \frac{\partial^2 \Gamma}{\partial \phi_1^2} = \frac{1}{S(q=0)} \tag{2}$$

N_i: weight average degree of polymerisation of component i

The interaction function Γ is related to the interaction parameter χ by:

$$\Gamma = \chi \cdot \phi_1\phi_2 \,. \tag{3}$$

During the intermediate stage both the wavelength and amplitude of concentration fluctuations change. During the late stages the concentration fluctuations are identical to the equilibrium composition of the co-existing phases, while the size of the domains still increases with time t. During the late stages both the maximum of the structure factor $I_m(t)$ and $q_m(t)$ are exponential functions of time [1–3, 16] with scaling exponents α and β:

$$q_m(t) \propto t^{-\alpha} \tag{4}$$

$$I(q_m(t) \propto t^{\beta} \,. \tag{5}$$

A scaled structure factor $F(x, t)$ is defined in the following way [1–3, 5, 16].

$$F(x, t) - I(q, t)\, q_m^d(t) \,, \tag{6}$$

with $x = q/q_m(t)$ and $d = 3$ (for a three-dimensional system). In the late stages $F(x, t)$ becomes independent of time, i.e., all $F(x)$ fall onto one master curve and $\beta = d\alpha$.

From Eqs. (1) and (2) it follows that $q_m(0)$ can be calculated if the temperature dependence of the interaction function Γ as well as the average segmental length σ and the degrees of polymerisation N_i are known. To compare the spinodal decomposition of different temperature jumps or different systems, it is useful to define a reference or critical time t_c which allows for a normalization of the absolute time scale by using t/t_c instead of t. t_c is defined by the time a particle needs to move across a distance of the correlation length $2\pi/q_m(0)$ [3, 6, 9].

$$t_c = \frac{1}{D_{app}\, q_m^2(0)} = \frac{1}{4\kappa} \cdot \frac{1}{M \cdot q_m^4(0)} \,. \tag{7}$$

However, besides t_c and $q_m(0)$ other shift factors A and Z can be used to create a master plot of reduced values for $q_m(t)$ versus t. This is done by choosing arbitrarily a reference temperature and then shifting the other curves both vertically ($\ln(Z)$) and horizontally ($\ln(A)$) onto it to yield

the best coincidence [9]. The shift factors depend on the chosen reference temperature.

The two shift factors A and Z are related to quantities proportional to the apparent diffusion coefficient D_{app} and the mobility M, D'_{app} and M' respectively.

$$A = \frac{1}{D'_{app} \cdot Z^2} = \frac{1}{M' \cdot Z^4} \tag{8}$$

A and Z rather than t_c and $q_m(0)$ need to be chosen when the early stages of spinodal decomposition cannot be resolved experimentally and the quantities of Eq. (7) cannot be determined. However, a transient curvature must be present in a plot of $\ln(q_m(t))$ versus, $\ln(t)$, since otherwise shift factors cannot be obtained unambiguously [9].

From an Arrhenius-plot of M' the activation energy of the uphill diffusion process can be obtained.

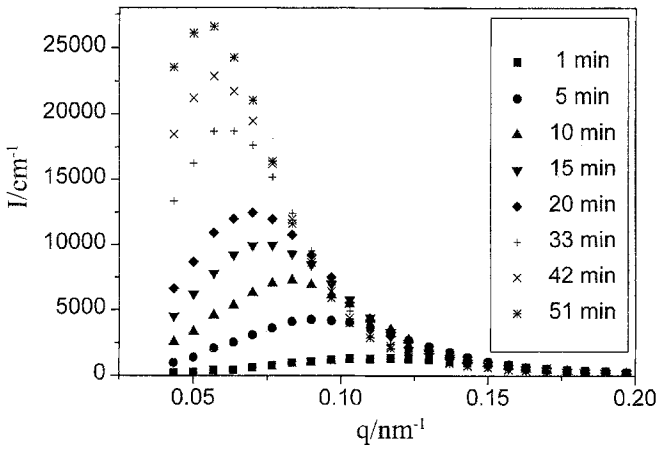

Fig. 1 SANS traces after a temperature jump from 30° to 12 °C

Results and discussion

Table 2 shows the glass transition temperature T_g of the blend during the first and second heatings. The sample was heated at a rate of 10 K/min from 223 to 413 K and annealed at 413 K for 10 min before cooling down again with a rate of −10 K/min. While during the first heating only one T_g is observed, during the second heating two T_g's are observed, which correspond to the pure components. This indicates a complete decomposition of the two components. Further, from this experiment one can conclude that the system does not undergo phase separation at room temperature (the DSC experiments were done ca. 2 years after sample preparation and the sample was stored at room temperature).

Figure 1 shows the scattering intensity as a function of scattering vector for various times after a temperature jump from the glassy state to 120 °C, as obtained from SANS. The scattering maximum position $q_{max}(t)$ and the maximum intensity $I_{max}(t)$ are shown as functions of time in Figs. 2a and b. From the slopes in the double logarithmic presentations it follows that the system is close to the late stages of spinodal decomposition ($\beta \approx 3\alpha$). The SANS curves show scaling behaviour of structure factors for the later times quite nicely, when plotted according to Eq. (6) (Fig. 3). From Fig. 3, one can conclude that in the regime of $q > q_m(t)$, a slope of approximately −4 is observed, which is the typical Porod-behaviour of two-phase systems with a sharp interface.

To create a master plot of $q_{max}(t)$ versus time of all data obtained by the three methods, they have to be shifted onto each other, yielding the shift factors defined in Eq. (8). Due to the absence of a pronounced transient curvature (i.e., intermediate stages) for most of our data (one example is shown in Fig. 2a), the vertical shifts are done by using $\ln(Z) = \ln(q_m(0))$ as calculated from Eq. (1). The necessary quantitites are given in Table 2. The error in such an analysis depends mainly on the distance of the system from the spinodal temperature. The further away the system is from the spinodal temperature, the less uncertainties in the χ-parameter influence the shift factor Z.

In Fig. 4 the master plot of all data obtained by SANS, DCD and SALS is shown, where 120 °C was chosen as the reference temperature. After shifting the data sets by the calculated $\ln(Z)$, also rather unambiguous shifting in the horizontal became possible to yield $\ln(A)$.

There are only a few temperatures at which all methods could be applied. A reason for this is the poor time resolution in the SANS measurements (at higher temperatures the evolution of the structure factor becomes too fast) and the long measurement times necessary for DCD. In spite of

Table 2 Glass transition temperatures, χ-parameter and statistical segment length of the blend

T_g[K] 1. Heating	T_g[K] 2. Heating	χ (from Ref. 8)	σ [nm] (from Ref. 8)
330	292 373	$0.022 \pm 0.01 - \frac{(6.9 \pm 3.0)K}{T}$	0.67

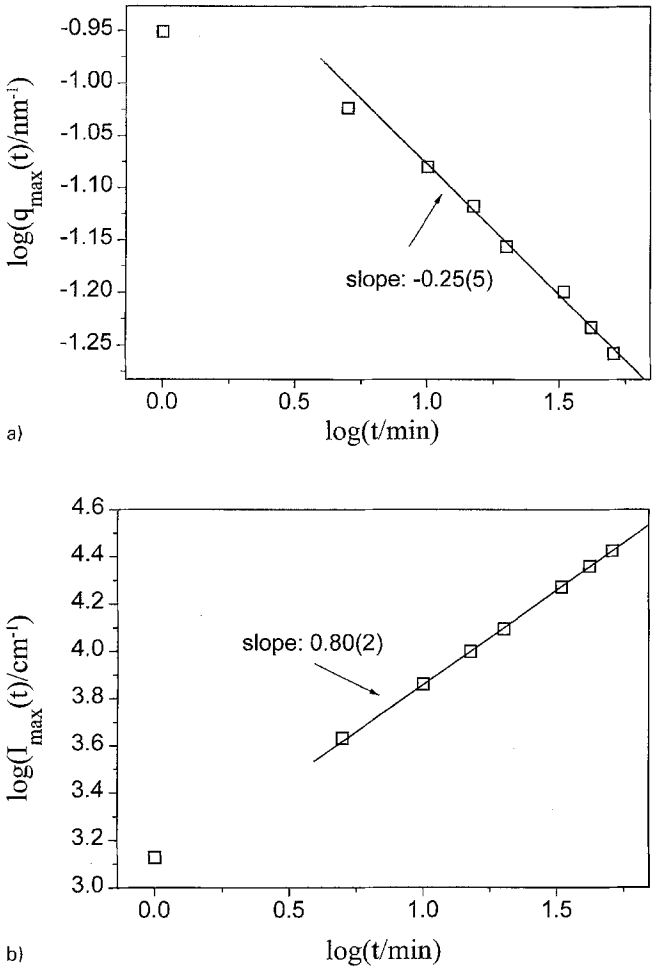

Fig. 2A Scaling behaviour of the spinodal peak position with time for a temperature jump from 30° to 120 °C. **B** Scaling behaviour of the spinodal maximum intensity with time for a temperature jump from 30° to 120 °C

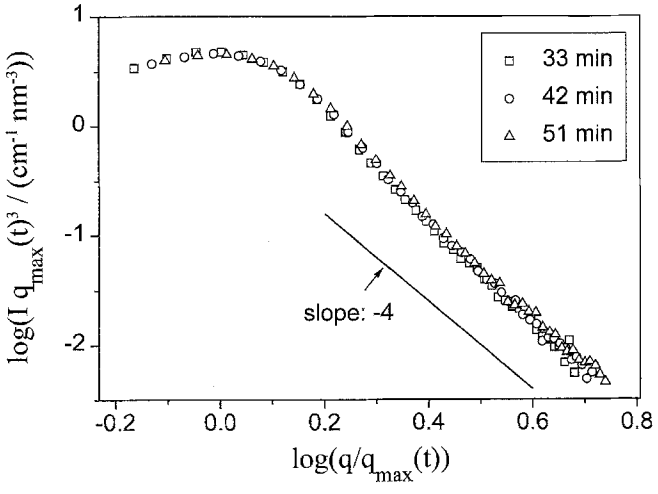

Fig. 3 Scaled SANS traces for a temperature jump from 30° to 120 °C at later times

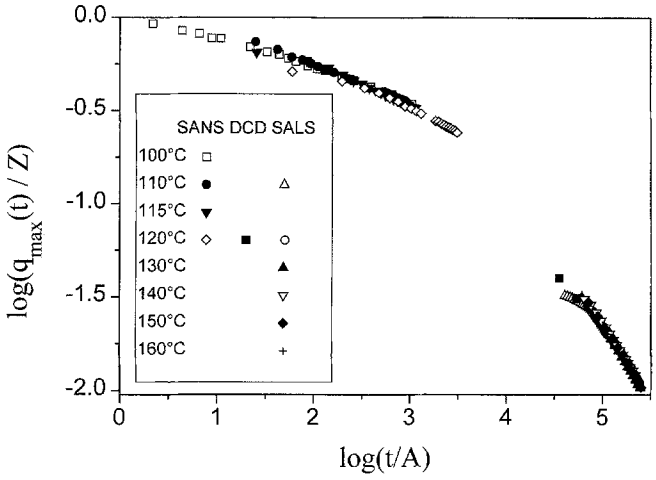

Fig. 4 Master plot of the scaling behaviour of spinodal peak position as a function of time at a reference temperature of 120 °C

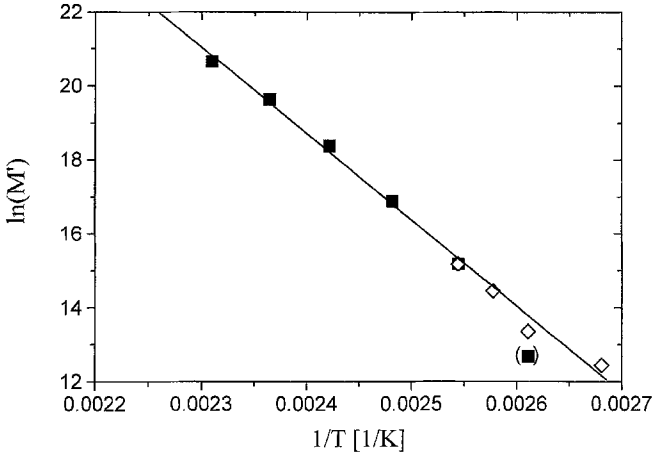

Fig. 5 Arrhenius-plot of mobility M': $E_A = 190$ kJ/mol is obtained from the slope of the linear fit (solid line); SALS data (■), SANS data (◇). The point in brackets was rejected from the linear fit

this experimental problem reasonable data for the mobilities M' from Eq. 8 are obtained. They are shown in Fig. 5 (Arrhenius-plot). It can be seen that both SANS and SALS data yield the same straight line, although the scaling behaviour, i.e., the exponent α is not the same for both data sets in Fig. 4.

From the slope the activation energy of the uphill diffusion process in this system can be calculated. An activation energy of ca. 190 kJ/mol is obtained for this system. This value unfortunately contains some uncertainty due to the fact that the χ-parameter also contains some error, as seen in Table 2. The activation energy can be compared with other results: Feng et al. investigated blends from polystyrene/poly(vinyl methylether) by temperature jumps within the single phase region (from a

temperature close to the spinodal temperature to temperatures deeper inside the single phase region by light scattering) and found $E_A \approx 80$ kJ/mol [17]. Best et al. investigated blends from polystyrene and poly(cyclohexyl methacrylate) by fluorescence densitometry and obtained $E_A \approx 268$ kJ/mol) [18, 19]. So the smaller activation energies are obtained for the systems with larger differences between glass transition temperatures T_g and the temperatures of the experiment.

Conclusions

It was shown that a scaling analysis of the later stages of spinodal decomposition over a wide scattering vector and time range gives access to the activation energy of the diffusion process. For systems showing only weak curvatures in the time scaling behaviour of the characteristic length of the system (as expressed by $q_{max}(t)$, the initial fluctuation wavelength can be used as one shift factor in the analysis, if it can be calculated from other data (χ-parameter etc.).

Since more often SALS techniques are available than for example SANS or small-angle x-ray scattering (SAXS), this way of analysis allows the investigation of the temperature dependence of dynamic quantities like mobility or interdiffusion coefficient in polymer blends which phase separate by spinodal decomposition, even if the early stages cannot be resolved by SALS.

Acknowledgments The authors thank Th. Wagner (MPI Polymerforschung) for the synthesis of the deuterated polystyrene, L. Noirez (CEN-Saclay) and P. Bellmann (GKSS) for their help during the small-angle neutron scattering measurements. The DSC curves were measured by G. Menk. The light scattering apparatus was setup by V. Edel (MPI Polymerforschung) and improved by U. Fasting (MPI Polymerforschung) and G. Müller (KFA Jülich). This work was mainly supported by the Bundesministerium für Wirtschaft (AiF-grant No. 7695), the Bundesministerium für Bildung und Forschung (grant No. FI3MPG) and by the EC Large Installation Programme. V.A. also gratefully acknowledges a fellowship from the EC Human Capital and Mobility Programme (No. ERBCHBICT930368).

References

1. Binder K (ed) (1991) Spinodal Decomposition. In: Haasen P (ed) Material Science and Technology, Vol. 5 VCH, Weinheim
2. Binder K (1994) Adv Polym Sci 112:181
3. Hashimoto T (1993) Structure of Polymer Blends In: Thomas EL (ed) Material Science and Technology, Vol. 12. VCH, Weinheim
4. Schwahn D, Jansen S (1992) Springer T, J Chem Phys 97:8775
5. Bates FS, Wiltzius P (1989) J Chem Phys 91:3258
6. Takenake M, Izumitani T, Hashimoto T (1992) J Chem Phys 97:6855
7. de Graaf LA, Möller M (1995) Polymer 36:3451
8. Schubert DW, Abetz V, Stamm M, Hack T, Siol W (1995) Macromolecules, 28:2519.
9. Abetz V (1994) Macromolecules 27:4621
10. Abetz V, Macromolecules, submitted
11. Cahn JW, Hilliard JE (1958) J Chem Phys 28:258; 1959, 31:668
12. Cook HE (1970) Acta metal 18:297
13. Flory JP (1941) J Chem Phys 9:660; 1942, 10:51; 1944, 12:425
14. Huggins ML (1941) J Chem Phys 9:440
15. Staverman A (1941) J Rec Trav Chim 60:640
16. Furukawa H (1985) Adv Phys 34:70
17. Feng Y, Han CC, Takenaka M, Hashimoto T 1992) Polymer 33:2729
18. Best M, Dissertation, Mainz 1991
19. Best M, Sillescu H (1992) Polymer 33:5245